

Neutron Generator System Design Report for CERN

**for
Dr. Christian Regenfus, University Zurich, CERN**

**as Deliverable Document
for first progress payment in accordance with
CERN's Price Enquiry DO-25627/PH dated 4-8-2008
and CERN purchase order CA 1491984**

**prepared by
J. Sved, NSD-Fusion GmbH
in collaboration with
Dr. John B. Fitzgerald, consultant**

**Doc. No. NSD-188
Date: 7-12-2008
Issue: 1, Version: B DRAFT**

This Document is of German origin and is copyright NSD-Fusion GmbH 2008. It contains proprietary information that is disclosed for Information purposes only. The contents of the document shall not, in whole or in part, (i) be used for any other purposes; (ii) be disclosed to any member of the recipient's organization not having a need to know such information or to any third party individual, organization or government or (iii) be stored on any retrieval system or be reproduced or transmitted in any form by photocopying or any optical, electrical, mechanical or other means without proper written permission of The Directors, NSD-Fusion GmbH, Falkenstrasse 3, 27755 Delmenhorst, Germany.

Tel +49 4221 924 926 Fax +49 4221 924 927 info@[nsd-fusion.com](mailto:info@nsd-fusion.com) www.nsd-fusion.com

Table of Contents

1	Introduction.....	4
2	NSD Neutron Generator Overview.....	5
2.1	Neutron Generator Set.....	5
2.2	IEC Fusion.....	6
2.2.1	Fusion Zone.....	8
2.2.2	Neutron Yield.....	9
2.2.3	Sealed Reaction Chamber.....	10
2.2.4	Temperature Control	11
2.2.5	Tritium.....	12
2.2.6	Transport Container Classification.....	13
2.2.7	Chamber dimension characteristics.....	15
2.3	Central Control Unit.....	16
2.3.1	Operations Sequence.....	16
2.3.2	Software Engineering.....	19
2.4	High Voltage Power Supply Unit.....	20
3	Shielding System.....	24
3.1	Concept.....	24
3.2	Reaction Chamber Construction.....	25
3.3	Vertical Support Sub-system.....	26
3.4	Mobility Requirement.....	27
3.4.1	Allowable Dimensions.....	27
3.4.2	Mobility.....	27
3.4.3	Base Design	29
3.4.4	Top of housing equipment.....	30
3.5	MCNP Model.....	31
3.5.1	MCNP Model Geometry.....	31
3.5.2	MCNP Material Definitions.....	31
3.5.3	Candidate Materials for the Radiation Shield.....	32
3.5.4	Dose Rate Simulation Results.....	36
3.5.5	Bremsstrahlung.....	42
3.5.6	Shielding Radiological Study Conclusions.....	43
4	Conclusion.....	44

Configuration Control

<i>Issue</i>	<i>Version</i>	<i>Date</i>	<i>Comment</i>	<i>Sections added</i>
1	A	2 Nov, 2008		
1	B	7 Dec. 2008		Radiation Transport

1 Introduction

The research team led by Dr. C. Regenfus at CERN has stipulated a Design Report regarding the neutron generator with movable radiation shielding housing and neutron area dosimeter interlock system.

This document is the deliverable Design Report.

Its focus topics are as follows:

- MCNP model analysis of the neutron generator induced radiation field within and external to the shielding.
- Mechanical characteristics of the mobile shielding sub-system
- Interlock safety features of the neutron generator control system

2 NSD Neutron Generator Overview

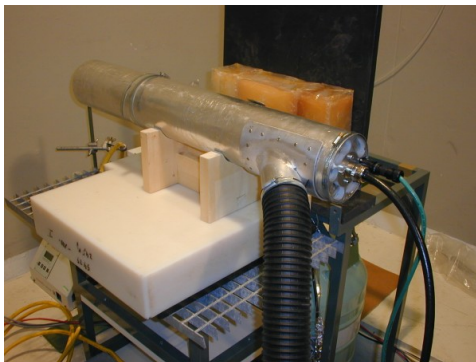
2.1 Neutron Generator Set

The NSD-Fusion Neutron Generator family includes a range of performance and configurations.

The NSD-NG-1E7-DD-C unit has a DC high voltage power supply rated at 120 kV, 15 mA maximum (1.8 kW).

This power is put into a glow discharge plasma load contained within the reaction chamber. The gas is Deuterium. This results in dd fusion and the emission of 2.5 MeV neutrons.

The neutron output is effectively regulated by an automation control computer. The user interface is via a LAN connection to a PC running a web browser which is Java enabled. Security functions are included.



2.2 IEC Fusion

The history of the NSD neutron generator technology is a branch of the history of Inertial Electrostatic Confinement (IEC) fusion research.

The famous inventor of television in the USA, Philo Farnsworth, also invented and named the IEC fusion concept (aka Fusor). In the late 1950's and 1960's he and a physicist R.L. Hirsch developed devices to attain higher fusion rates by the DD and the DT reactions. These were spherical geometry reaction chambers with a spherical central grid electrode.

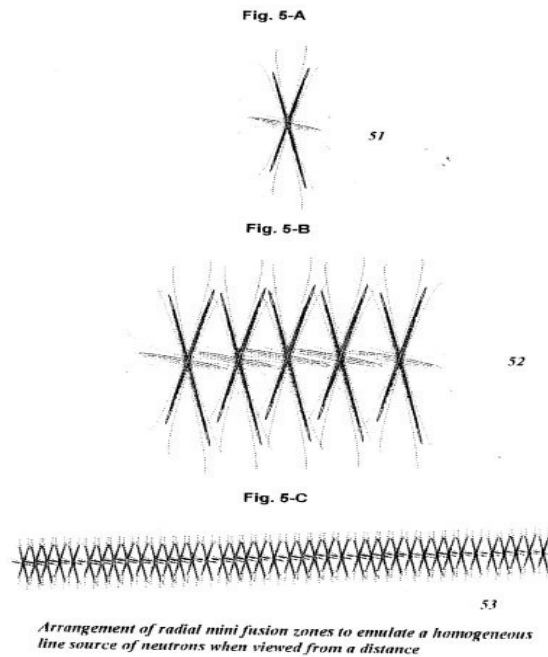
The concept is a simple gas discharge at low pressure of approximately 10^{-2} mbar. The DD or DT gas will break-down with the application of a voltage in the range 10 – 100 kV. In a steady state continuous power mode the plasma will be of a glow discharge type. Unlike classic parallel plate measurements and theory, the hollow cathode central electrode and outer anode topology defines a symmetric electrostatic field. The trajectory of a positive charge ion such as D^+ or T^+ or charged molecules of DD, TT, DT is such that it will generally be attracted toward the central cathode. The cathode is a cage-like structure with thin vane elements aligned radially. It is therefore apparently transparent in the local radial direction. Most ions pass through the cathode grid without colliding with it. Some ions born near to the cathode grid will collide with it. In the relatively high number density gas-plasma mix at 10^{-2} mbar a single ion will undergo charge exchange collisions with other ions and neutrals. The research literature indicates that this is an energy loss process that reduces the energy available for acceleration of ions to high kinetic energy where fusion grade collisions occur. It may never attain fusion power but it is fine for longest life industrial or research neutron generators.

The application of energy is via the glow discharge voltage and current. The current is limited by the power supply. A glow discharge will conduct as much current as can be provided and is said to have an inverse resistance. The applied current determines the ion population. The scaling of fusion collision rate with applied voltage and current has been measured by several fusion research groups in the USA and Japan. The scaling is proportional to $V^{3.3}$ and $I^{1.3}$ according to recent experiments in Japan and $I^{1.5}$ according to more recent experiments by the University of Wisconsin which both utilize a pulsed power supply strategy with a spherical reaction chambers which have less specific performance than the NSD neutron generator. NSD-Fusion will verify the scaling factor. With pulsed power a high voltage and high current are applied as a pulse. In the short period of the pulse the current that can be delivered to the plasma load can be 10 or more ampere. The super linear proportionality means that there is a higher rate of fusion neutron emission than in a steady state DC power supply of comparable power.

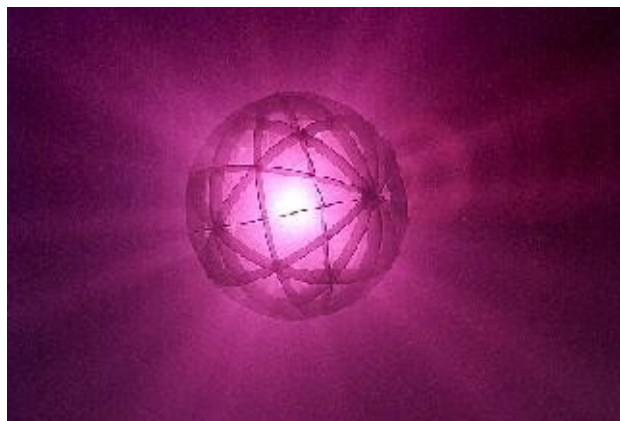
The input power, operating temperature and waste heat transfer are significant engineering considerations. The use of pulsed high voltage provides more specific performance and also reduces the potential for electrode arc damage. The thermal capacity or ability to radiate heat is an engineering limit. NSD will complete high temperature resistant electrode tests in order to determine the design limit for the cathode grid. This is expected to allow 1 kW or more per 25 mm of electrode length. High heat transfer with a water cooling loop plus high temperature Tungsten electrode are expected to allow the specific power to be increased. This will reduce the total length of the electrode.

The NSD experience with IEC devices has been to develop industrial grade automated robust neutron generators rather than experimental laboratory experiments built from vacuum components and power supplies that are not well suited to the requirements of the device. NSD equipment is built for the specification and is can be frequently operated rather than just displayed to visitors.

The diagram below illustrates the topology of the NSD reaction chamber.



The compound alignment of electrode cells produces an almost homogeneous zone of fusion neutron emission along the length of the electrode. The star beams of electrons are aligned with the openings of the electrode. Electrostatic lens and ion kinematics drawing the oscillating particles in the star beam channels. The electron beams carry a significant fraction of the power to the vessel wall. The electrode is a cathode and becomes hot enough for thermionic emission of electrons. The electrical energy becomes parasitic heat. The absence of a solid target spot and electron beam spots avoids very intense localized heating.



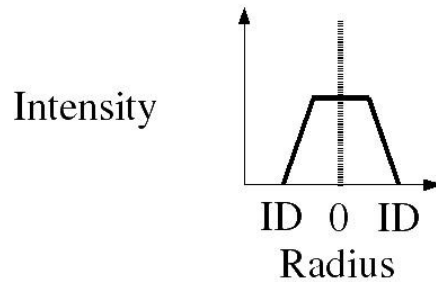
Spherical Mk0 neutron generator IEC fusion zone. (copyright NSD-Fusion GmbH)

For fast neutron radiography, the star beam or spoke and hub topology of linear geometry NSD neutron generator neutron origin may be used with deconvolution techniques. The in another electrode configuration a planar electrode consisting of an array of cells in each of which a single star topology is established, the use of cell blocking components can be used to construct a coded array of sources. Similar to coded aperture deconvolution techniques, the neutron generator provides a coded source pattern but without a mask.

2.2.1 Fusion Zone

The fusion zone, where neutron emission reactions occur, is postulated to be as described below.

The neutron metrology department of the PTB Braunschweig, Dr. Klein, made measurements of the spherical Mk0 reactor chamber which indicate that the neutrons are emitted with an intensity distribution as shown below.



The intensity distribution within the linear reaction chamber is assumed to be similar. The plateau may correspond with the diameter of the central electrode. However this is not known. It may extend beyond the volume of the electrode. The plateau may be strong evidence that the formation of potential wells, often postulated for Inertial Electrostatic Confinement fusion, is not occurring in the operating regime of relatively high gas pressure. The flatness of the plateau has not been quantified.

The increase in intensity towards the center is driven by the volumetric concentration of energetic ions and neutrals. There are many plasma mechanisms which may be considered. Most likely the ramp is not linear.

A limiting value of fusion rate may be zero at the inside wall of the chamber. However there may be some DD fusions between particles in motion and static particles in the metal matrix of the wall.

FIG. 2A

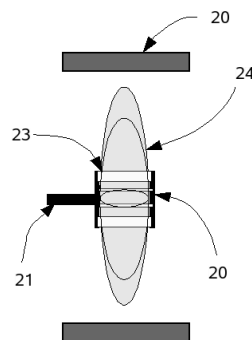
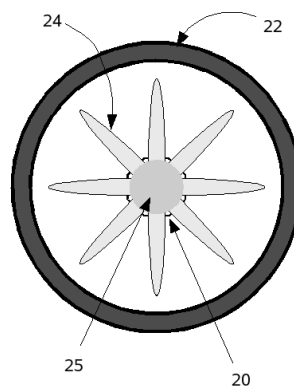


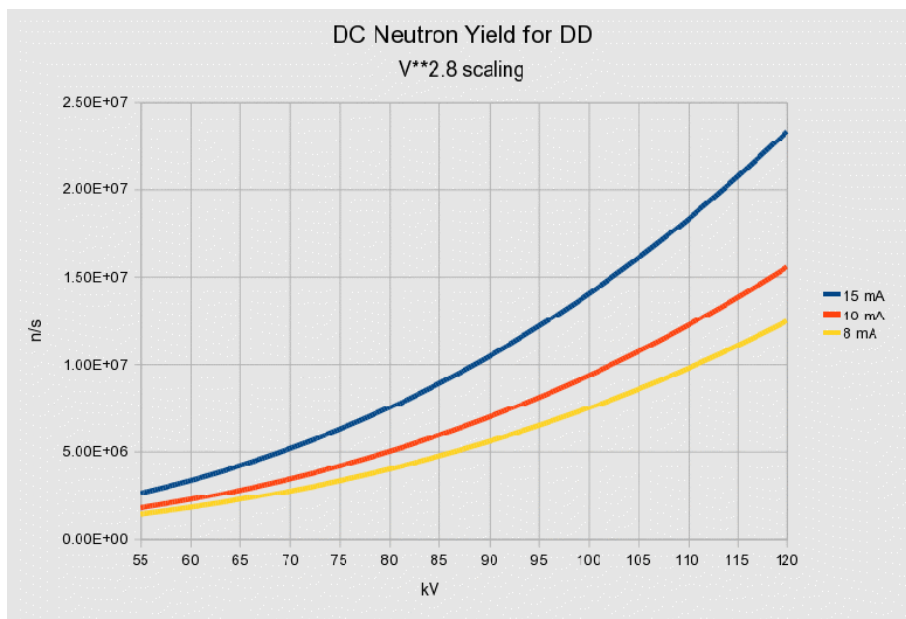
FIG. 2B



A postulated structure of the neutron origin or emission zone is shown above. The spoke like structure plus a more intense central zone may exist. Experimental measurements are planned to map the neutron emission topology.

2.2.2 Neutron Yield

The blue line in the chart below shows the performance of the deliverable neutron generator model NSD-NG-1E7-DD-C. This unit has a 36 mm long electrode which is matched to the maximum input power of 1.8 kW.



2.2.3 Sealed Reaction Chamber

The reaction chamber assembly consists of a hermetically sealed vacuum vessel.



The Ultra High Vacuum seals are used in many vacuum systems including particle accelerators. Residual Helium leakage is less than 10^{-10} mbar.l/sec . At such a leakage rate the reaction chamber will retain operational conditions for a decade or longer.

In the event that reaction chamber servicing is required, the fill port can be opened. It is re-usable. Servicing is offered by NSD-Fusion.

The entire reaction chamber is housed within an aluminium cylinder which has a cowling to direct the cooling air flow across the cooling fins.

2.2.4 Temperature Control

The "source" is the plasma with fusion grade collisions. It has a temperature of perhaps 20-30°C when operating.

The electrons emitted by the ca. -100 kV electrode cause heating of the vessel wall (and Bremstrahlung x-rays). The wall is also a heat exchanger (via the cooling fins). An equilibrium is usually achieved with a moderate air flow so that the base of the fins have a temperature of about 90°C. The outer casing or cowling has a temperature of about 30°C while the air is flowing.

The hot electrode will have a temperature of ca. 1000°C. But it has a low mass, say 50 gram.

The hot getter pump has a temperature of 500°C. It is insulated by the vacuum and by an internal thermal cover. So it only needs 8 W to remain at operating temperature. When getter pump heater is switched off, it takes more than 30 minutes to cool down to ca. 100°C (asymptotic).

IF the full powered NSD neutron generator suffers a cooling fan failure (no cooling air) the temperature will rise. A limit value for the cooling fin root temperature will be exceeded and the automated control will stop the high voltage and issue a warning or explanation message.

A simple calculation may be as follows.

Assume 1 kg of Aluminium. At 120° C versus 20°C this has a thermal energy increase of 8.97E4 J (specific heat of Al 24.2 J/mol.K)

Assume a cylinder of Paraffin 1 cm thick in contact with the Al body 0.3 m x 1.3 m diameter
=> 1.23E-3 cub.m of wax

For a 30 °C rise from 20 to 50°C melting point 7.31E4 J is required.

So the heat from the hot reaction chamber (not being cooled by flowing air) could in this very simple model transfer to the adjacent wax and heat it to above melting point.

However, the reality of heat transfer is that there are:

insulation effects,
other parts absorbing the heat and conducting it away (e.g. lead shielding)
and general dilution by all of the mass not considered above.

This means that it will be very difficult to locally heat the Paraffin or similar shielding material to the point where it would melt.

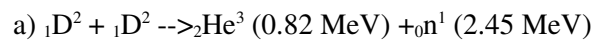
Reaction chamber cooling is achieved by a variable speed centrifugal air blower. The 240 Volt DC motor speed controlled via a 0-10 volt control signal from a PID control loop. Therefore the target reaction chamber wall temperature is maintained. When the neutron

generator is operated at lower than maximum output the air blower speed will also be reduced. This will mitigate air blower noise.

2.2.5 Tritium

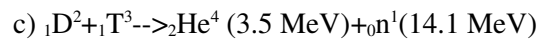
The Deuterium Deuterium fusion reaction will produce Tritium and Helium 3 nuclei at the same rate as neutron production.

The following fusion reactions predominate.

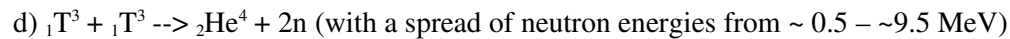


reactions a) and b) occur with equal probability.

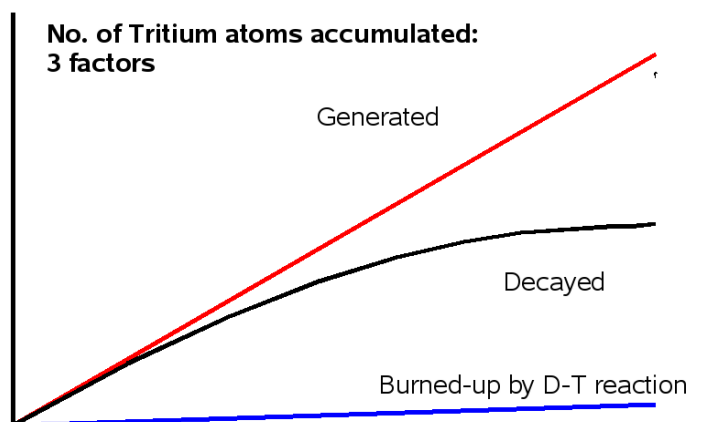
OR in the case of DT mix



OR in the case of Tritium only mix



In a DD neutron generator such as the unit to be delivered under CERN purchase order number CA 1491984, the accumulated or generated T will remain insignificant for the generation of 14 MeV neutrons from a 2.5 MeV DD neutron generator.



The above chart shows the Tritium accumulation factors. Decay is significant but burn-up is more effective in elimination of the accumulated Tritium.

So the produced and actually accumulated amount of Tritium remains well within the free limit of 400 GBq. A DT 14 MeV version of the NSD-NG will be loaded with Tritium to near to the 400 GBq limit. The DD 2.5 MeV version of the NSD-NG which is considered here may generate perhaps a few GBq of Tritium that will exist for any long period.

During early testing and the initial running in phase, the low pressure is established by means of a vacuum pump unit which exhausts to atmosphere. The emission of T from the vacuum unit at the possible rate of production remains below permitted levels.

A DT 14 MeV version of the NSD-NG will be loaded with Tritium to near to the 400 GBq limit.

2.2.6 Transport Container Classification

Two scenarios are considered:

- A Deuterium filled reactor chamber assembly will accumulate Tritium through its use as a neutron generator.
- A Deuterium-Tritium filled reactor chamber will lose Tritium through its use as a neutron generator.

The greatest amount of Tritium occurs in the DT version at the time of filling.

The case of the Deuterium filled reactor chamber will not achieve the same level of Tritium activity after a maximum practical working lifetime.

Therefore a classification for the case with the greatest amount of Tritium will cover all other scenarios of usage and transportation.

During transportation the Tritium is stored in solid solution within a getter pump material. The Tritium is incorporated into the instrument. The instrument remains hermetically sealed until it is returned for removal and replenishment of the reactant gas. The containment vessel is shown to be of very robust construction which can easily assure safety during minor mishaps and many accident conditions.

The typical Tritium activity level is 140 GBq or 280 GBq (or 420 GBq) as determined by the number of getter material units used. The limit is set by the allowable limit value of 400 GBq

based on the IAEA Regulations for the Safe Transport of Radioactive Materials 1996 Edition
(Revised) No. TS-R-1 (ST-1, Revised)

Therefore the classification as a transportation package is:

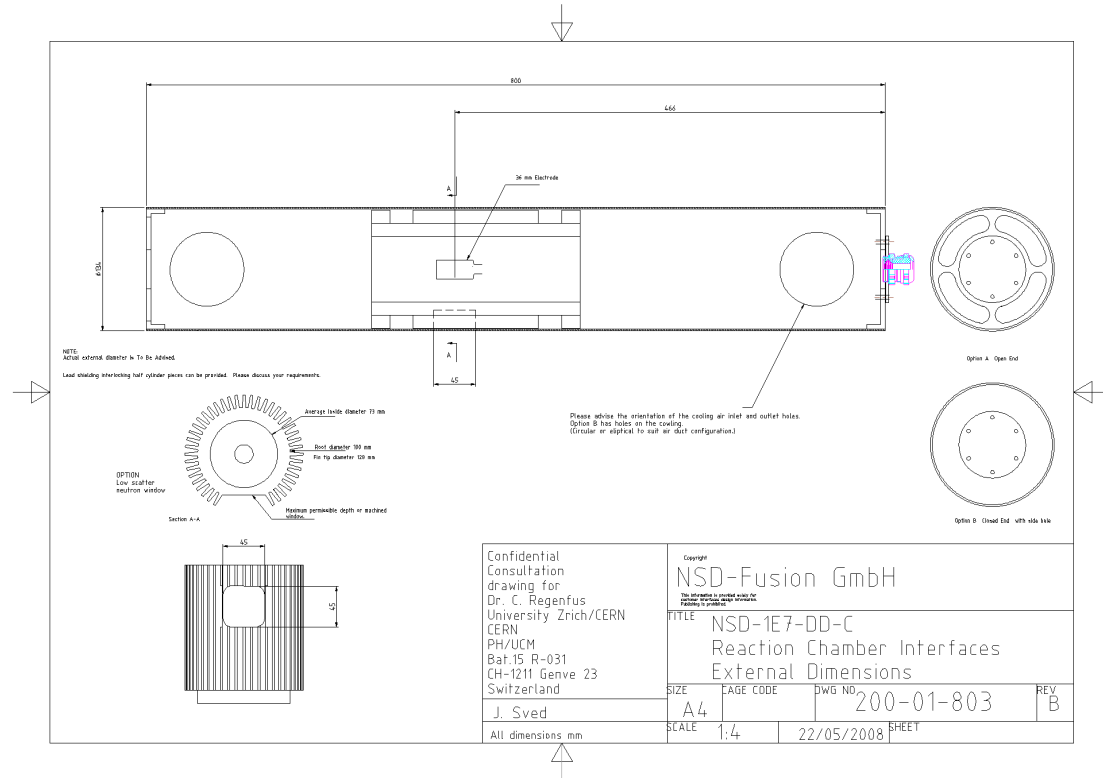
Class 7

UN2911

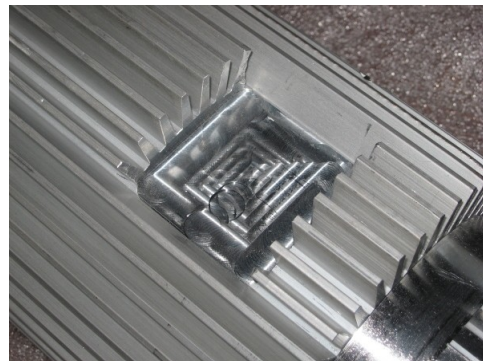
This also satisfies the USA NRC Regulations

Title 49 CFR Part 173.421 for excepted radioactive material.

2.2.7 Chamber dimension characteristics



The mass of a short reaction chamber assembly is 15 kg.



The above photos show the minimised neutron scatter "window".

2.3 Central Control Unit

The automation platform is a Beckhoff CX10x0 Industrial PC with appropriate input/output modules for the neutron generator functions.

The DC High Voltage power supply is also accommodated in the same small rack enclosure as pictured.

The operator of the neutron generator first powers IPC unit on via the front switch.

After 30 seconds the software is boot loaded and operational. This is indicated by the green LED.

The control interface is a web browser with Java installed on another PC. Any common operating system is therefore supported after the open source TightVNC client application is downloaded and installed. The IP address and port are called via the web browser and then a window which contains the virtual control panel is opened. A secure link is established by a log-in procedure so that only the operator's PC can be in interactive communication with the neutron generator controller.

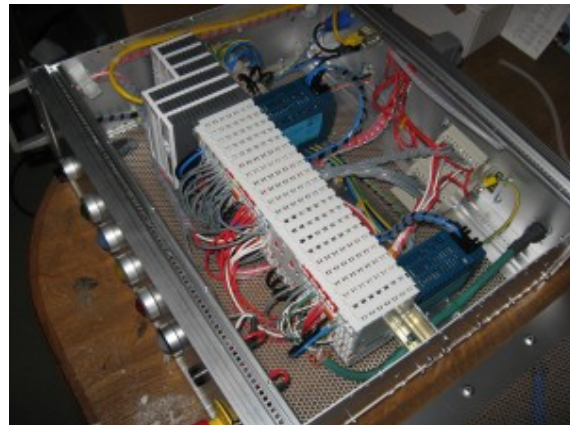
Observers can also log onto the VNC server, but there will be no command capability. This may assist logging functions.

2.3.1 Operations Sequence

The operator selects the warm-up button on the virtual control panel. The getter pump heater temperature is gradually increased over about 10 minutes. During this phase the blue LED is at first constantly ON when the getter temperature is cold. As the heating progresses the Yellow LED flashes at an increasing rate to indicate that the heat-up is progressing. When the getter temperature is warm (about 250°C) the blue LED goes OFF. When the Getter Heater is at about 500°C the Yellow LED remains continuously ON. After a predetermined waiting period which ensures



NSD Central Control Unit and 1.8 kW DC HV PSU enclosure. A typical industrial PC and its I/O modules plus power switching relays and 24 volt DC power supply can be accommodated in a 3U 19" sub-rack or similar enclosure.



Connections: Data, Temperature, Heater Power, Interlocks, Warnings, HV PSU monitor and control, relay switched mains power out, mains power in.

that the gas pressure has stabilised, the neutron generator reaction chamber is ready to be operated.

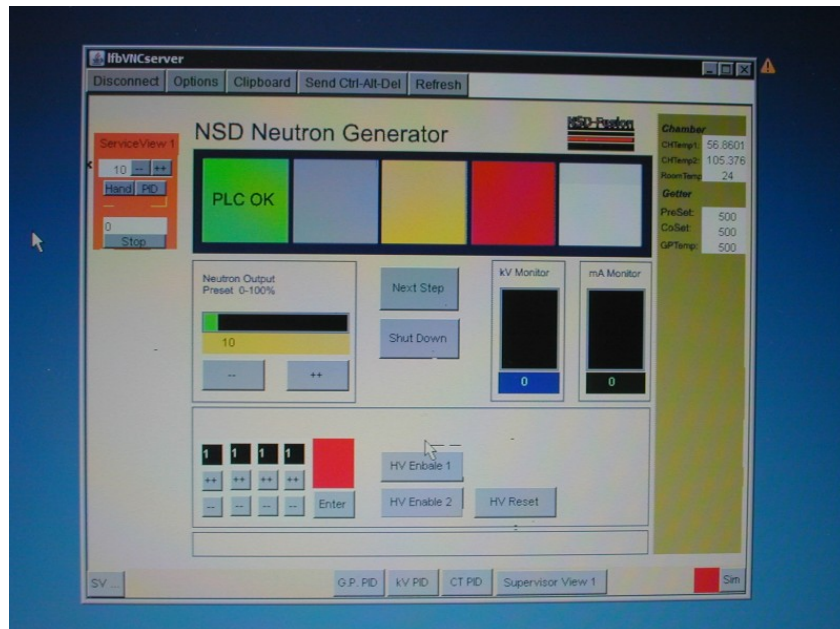
Operation of the high voltage power supply is only permitted when the door and emergency stop interlock circuits are closed.

The HV power supply requires the HI signal (24 volt) directly to close the internal relay.

The automation also requires the HI signal from the door and emergency stop circuits before it will issue the two high voltage enable signals which are also required by the high voltage power supply.

The High Voltage can be stopped manually by pressing the HV Stop button or the Shutdown button on the virtual control panel. Pressing a physical Emergency Stop button also immediately inhibits the High Voltage and hence radiation emission.

A second press of the Shutdown button will prompt a Accept or Cancel message. Acceptance will cause the getter pump heater to be switched off. After this the CCU will continue to monitor the reaction chamber temperature and operate the cooling air blower if necessary until the automation computer is switched off at the front panel main switch.



The absence of front panel control switches on the HV PSU and CCU prevents independent command inputs.

The CCU and PSU will be located close to the neutron emission unit. A 15 m high voltage cable is provided.

The location of the control operator can be anywhere with Local Area Network connection. Internet external world connection is NOT recommended as it may be a security risk.

It is up to the operators of the neutron generator to determine the safety practice and configuration in accordance with ALARA criteria. The NSD neutron generator system provides flexibility.

Please refer to the user manual for more details about the monitor and command interface as well as the functions of the automation software.

When the generator of neutrons is wanted, the command input by the operator causes the check of door switch and emergency stop interlocks. This circuits connect to J3 on the back panel of the CCU.

DSWP	DoorIntl
EmStP	EmStop
VentEN	Dosi1
Caution	Dosi 2
Acoustic	Dosi 3
Operate	Dosi 4
Alarm	0V
0 V	0V

J3 connections

Note the Neutron Dosimeter lines which are available.

The front panel main power switch on the HV PSU must be in the ON position but the HV PSU will not become active because of the still open mains power relay in the CCU.

Then the mains power relay to the HV PSU is closed when the software is satisfied that all door and emergency stop interlock signals are HI. Then the HV PSU comes online.

Simultaneously relays will close for auxiliary external indicator devices connected to J3 on the back panel of the CCU. These include the 24 volt signal for warning lights.

On the front panel and the virtual control panel the RED LED will initially flash when the HV PSU is powered via the mains relay in the CCU. When the HV is enabled the RED LED will be continuous.

An audio alarm unit will also emit sound to warn that the HV PSU has been activated. It will again warn when high voltage is enabled.

A White LED provides an indication when the Emergency Stop or Door switch is opened.

The audio alarm will again emit a signal when such an event occurs.

Various fault monitoring functions in the HV PSU become active. An faults are indicated to the CCU software via dedicated lines in the umbilical cable.

If all safety conditions are satisfied, the software presents the operator with the virtual High Voltage enable switches. With both switches enabled High Voltage power will be delivered to the reaction chamber.

The software monitors the immediate plasma "ignition" and configures the system for normal regulation to achieve the pre-set target values of plasma voltage and current.

The plasma current is regulated by the HV PSU taking a target value from the CCU software.

The plasma voltage is regulated by the CCU software. This regulates Getter Pump temperature with determines the plasma voltage.

In the event of "mini-arcs" the CCU software determines if an unsafe condition is present. Mini-arcs are a phenomenon during the initial running in of the reaction chamber. With the high quality electrodes there is actually little problem with residual particles in the reaction chamber.

The neutron generator will achieve the target operating conditions quite rapidly. As the control software evolves, the necessary "smarts" will be implemented to fully automate the rapid achievement of target operating parameters.

If the operator wants to switch off the neutron generation, the system will continue to maintain the standby conditions. The utilization of the door and emergency stop interlocks is recommended for the laboratory safety protocol. The HV PSU shall be commanded to go off-line and the CCU mains power relay will isolate the HV PSU.

The opening of a door switch or an Emergency Stop switch will also ensure that this condition is achieved.

Similarly the CERN required Dosimeter interlock can be added. As there are four interlock or alarm signals provided by the Bertholds LB111 neutron dosimeter these will be used to provide warnings to the operator and to automatically trigger the CCU software to take the HV PSU off-line in the event of a safety limit being reached.

It is the function and responsibility of the CERN radiation safety officer to set the alarm and limit values and to place the neutron detection unit in a position which is meaningful for personnel radiation protection.

The CCU software will respond to warning and alarm signals. One Dosimeter interlock channel will be configured to initiate an Interlock LO signal that will take the HV PSU off-line.

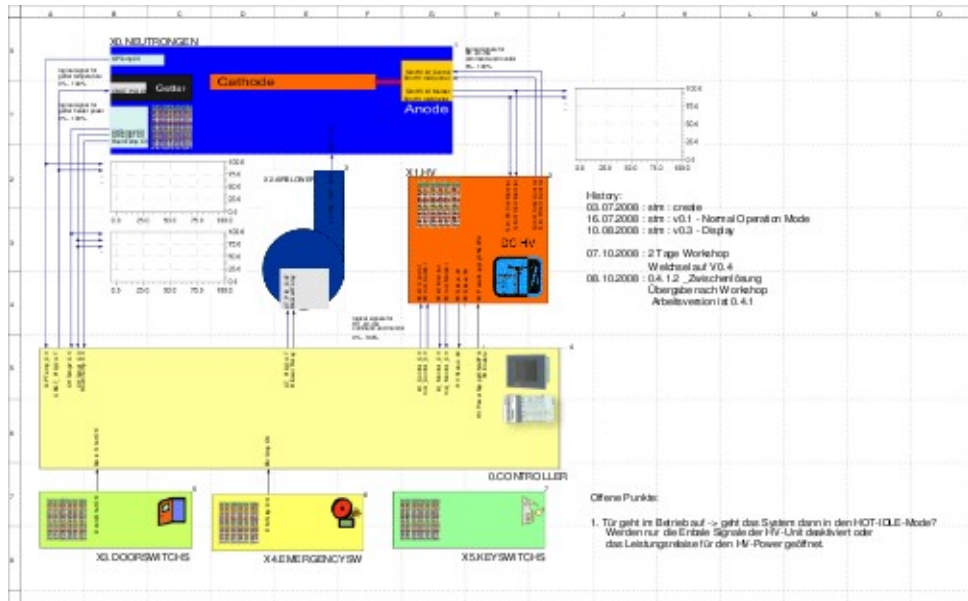
When operations are concluded, the operator can command the neutron generator to Shut Down. This will cut the Getter Pump heater power.

The air blower will continue to operate until the reaction chamber temperature is below a threshold value.

2.3.2 Software Engineering

The software has been developed originally for the defunct Mk0 neutron generator. The software requirements documentation has been used with modern structured software engineering techniques. These techniques are the foundation of a programming tool which is geared to support the CX10X0 industrial computer platform.

The software provides a hierarchical structure to burrow down to simple functional modules.



The screen shot above shows the top level.

Simulation has been a feature of the tool to enable program testing prior to the addition of the hardware. The testing facility allows a progressive build of the software according to the operational modes and states of the neutron generator system.

2.4 High Voltage Power Supply Unit

The High Voltage power supply is configured to only operate in conjunction with the Central Control Unit or with a manual control box that is used during the manufacturing and test phase.

The following pin-off list provides a brief overview of the control and monitor functions.

1	3PhaseApplied	INPUT	+24V = Command close contactor. 0V (or o/c) = Open contactor
2	0VPower/Logic		0V return for the logic input signals
3	HV_NoFault	OUTPUT	+24V = HVPSU fit to operate. 0V (is open circuit) = Fault present preventing operation.

4	HV_Monitor	OUTPUT	+24V = HV is ON at lowest internal command level (i.e. at PWM chip). 0V (is open circuit) = HV is held off.
5	HV_kVCtrl	OUTPUT	+24V = The output voltage is maintained. 0V (is open circuit) = The output voltage is indeterminate.
6	HV_mACtrl	OUTPUT	+24V = The output current is maintained. 0V (is open circuit) = The output current is indeterminate.
7	NoArcSensed	OUTPUT	+24V = Normal operation. 0V (is open circuit) = An arc has been detected - reset to clear.
8	3PhaseMon	OUTPUT	+24V = Contactor is closed. 0V (is open circuit) = Contactor is open.
9	HV_Enable1	INPUT	+24V = Activate HV (needs confirmation from enable 2). 0V (or o/c) = HV inactive.
10	HV_Enable2	INPUT	+24V = Activate HV (needs confirmation from enable 1). 0V (or o/c) = HV inactive.
11	-15VControlBox	OUTPUT	-15VDC low power source from HVPSU to provide power for references, etc. (~100mA available).
12	ArcDetectReset	INPUT	+24V = Clear the latched arc detection signal (line 7). 0V (or o/c) = Normal state.
13	+15VControlBox	OUTPUT	+15VDC low power source from HVPSU to provide power for references, etc. (~100mA available).
14	EmStopIntlk	INPUT	+24VDC input to HVPSU indicating emergency stop healthy. When logic 0, opens internal contactor in HVPSU
15	DoorIntlk	INPUT	+24VDC input to HVPSU indicating reactor door closed. When logic 0, opens internal contactor in HVPSU
16	HV_kVMonitor	OUTPUT	0-10V analogue signal to PLC Host representing actual HV output. 10V = 120kV.
17	0VAnalogueHV		0V reference output. Avoid current flow in this wire which will cause offsets.
18	HV_mAMonitor	OUTPUT	0-10V analogue signal to PLC Host representing actual mA output. 10V = 15mA.

19			
20	0VAnalogueRef		0V reference output. Avoid current flow in this wire which will cause offsets.
21	HV_kVComm and	INPUT	0-10V analogue signal to HVPSU defining the high voltage set point or maximum limit.
22	HV_mAComm and	INPUT	0-10V analogue signal to HVPSU defining limiting/demand output current
23	ExtWarningLampPOS	OUTPUT	Output to external warning lamp (+12V/5W only)
24	ExtWarningLampNEG	OUTPUT	Return from external warning lamp
25	ContactorLockout	OUTPUT	+24V = Normal operation. 0V (is open circuit) = Pulse indicating contactor is opened. This causes a delay before the contactor can be closed again. Prevents abuse of the contactor.
26	LampAlarm	OUTPUT	+24V = Normal operation. 0V (is open circuit) = The external warning lamp is failed at the same time as the contactor is requested closed. Signal inactive if contactor requested open.
27	Fan1OK	OUTPUT	+24V = Crossmember fan OK. 0V (is open circuit) = Fan fault detected.
28	Fan2OK	OUTPUT	+24V = Rear panel fan OK. 0V (is open circuit) = Fan fault detected.
29	Fan3OK	OUTPUT	+24V = Side panel fan OK. 0V (is open circuit) = Fan fault detected.
30	PFC1IOGOK	OUTPUT	+24V = PFC Module 1 indicates the output is good. 0V (is open circuit) = Not good.
31	PFC1ENOK	OUTPUT	+24V = PFC Module 1 Load Enable signal is good. 0V (is open circuit) = Not good.
32	PFC1IOGOK	OUTPUT	+24V = PFC Module 2 indicates the output is good. 0V (is open circuit) = Not good.
33	PFC1ENOK	OUTPUT	+24V = PFC Module 2 Load Enable signal is good.

			0V (is open circuit) = Not good.
34	Thermal_1OK	OUTPUT	+24V = The thermal switch 1 has not operated. 0V (is open circuit) = Overtemperature.
35	Thermal_2OK	OUTPUT	+24V = The thermal switch 1 has not operated. 0V (is open circuit) = Overtemperature.
36	LVPSU_OK	OUTPUT	+24V = All the internal low voltage power rails are good. 0V (is open circuit) = Power rail(s) out of spec..
37	Inverter1_O/C	OUTPUT	+24V = Normal operation. 0V (is open circuit) = Pulsed momentarily low to indicate that the current limit signal for inverter 1 has been activated.
38	Inverter2_O/C	OUTPUT	+24V = Normal operation. 0V (is open circuit) = Pulsed momentarily low to indicate that the current limit signal for inverter 2 has been activated.
39			Do not use (no mating terminal at PLC end)
40			Do not use (no mating terminal at PLC end)
41			Do not use (no mating terminal at PLC end)
42			Do not use (no mating terminal at PLC end)

3 Shielding System

3.1 Concept

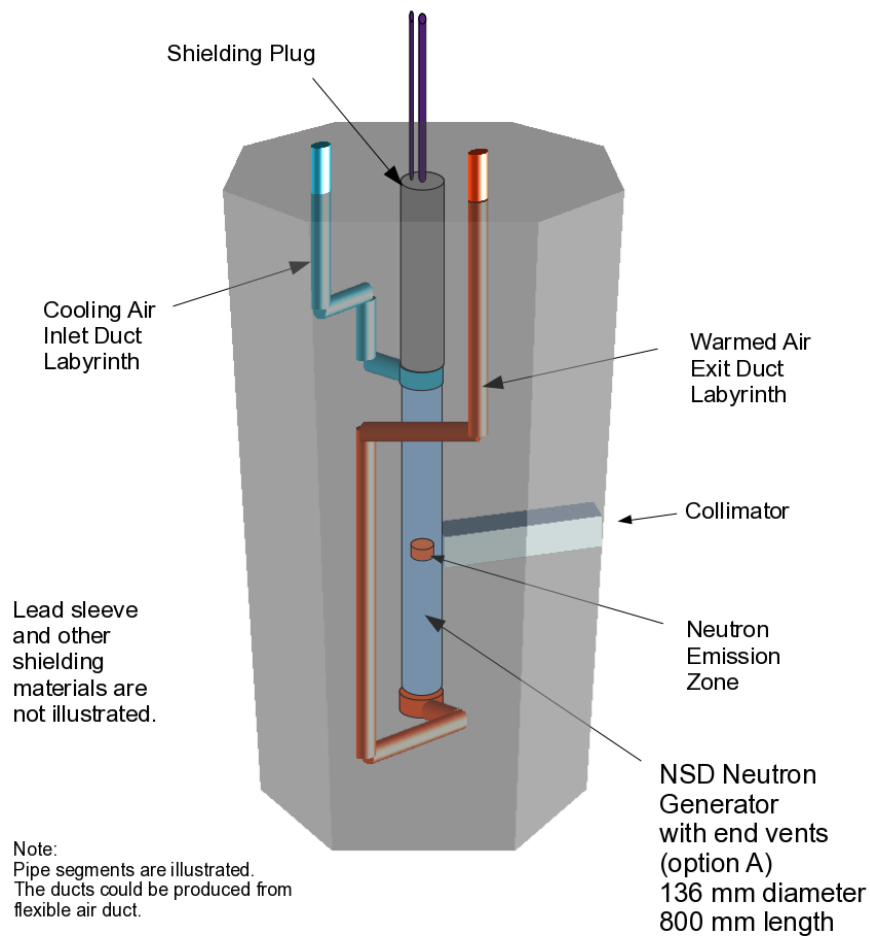
The diagram illustrated the basic concept.



J. Sved 19-05-2008
 supplied to Dr. Regenfus, CERN
 Prof. Strauman, University Zurich
 as confidential consultation information.

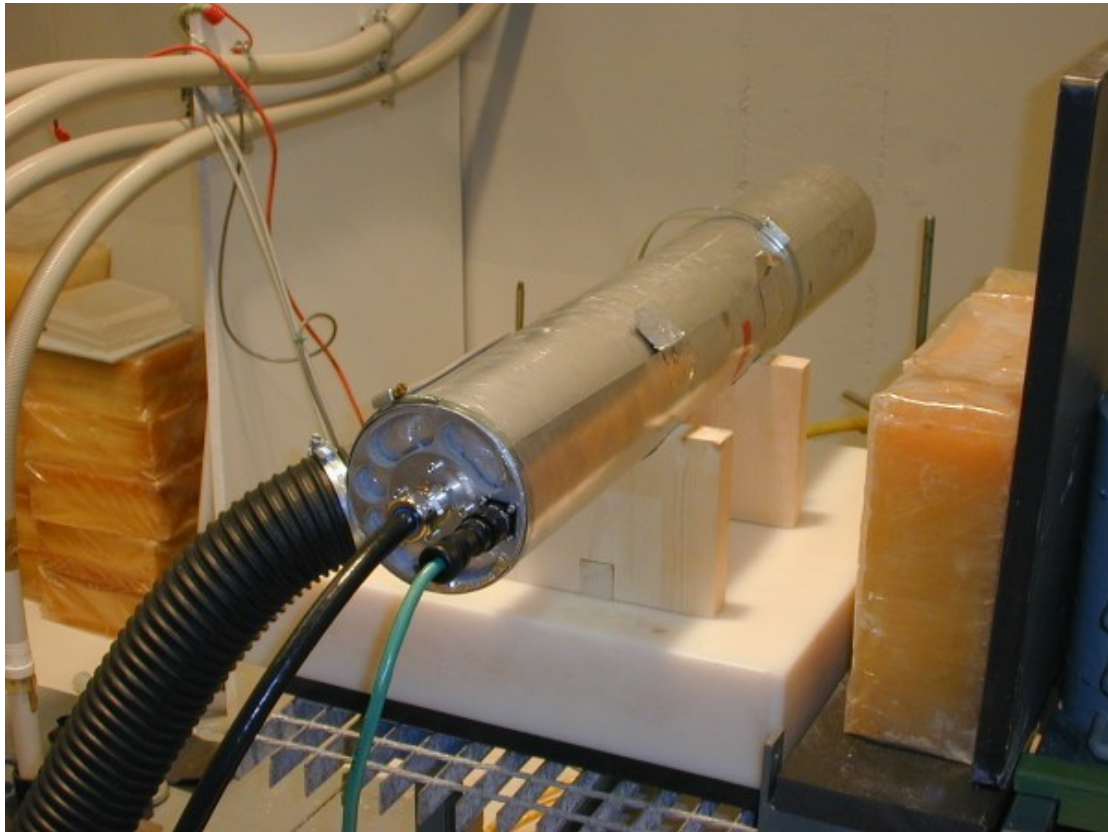
Concept for a mobile shielded enclosure

Specification required for residual emissions of neutron, x-ray and gammas versus neutron emission (n/s) or area dose at 10 cm from external surface.

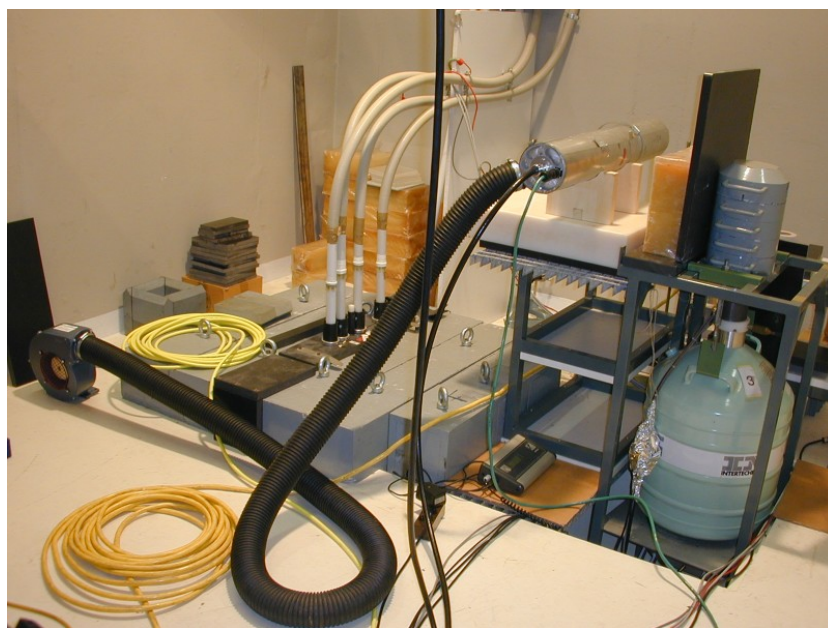


3.2 Reaction Chamber Construction

The photos below show aspects of the reaction chamber assembly.



The cooling air system is integrated into the shielded housing. In the photo above the cooling air is delivered from the variable speed blower via a hose and side entry fitting. The axial holes are blanked.

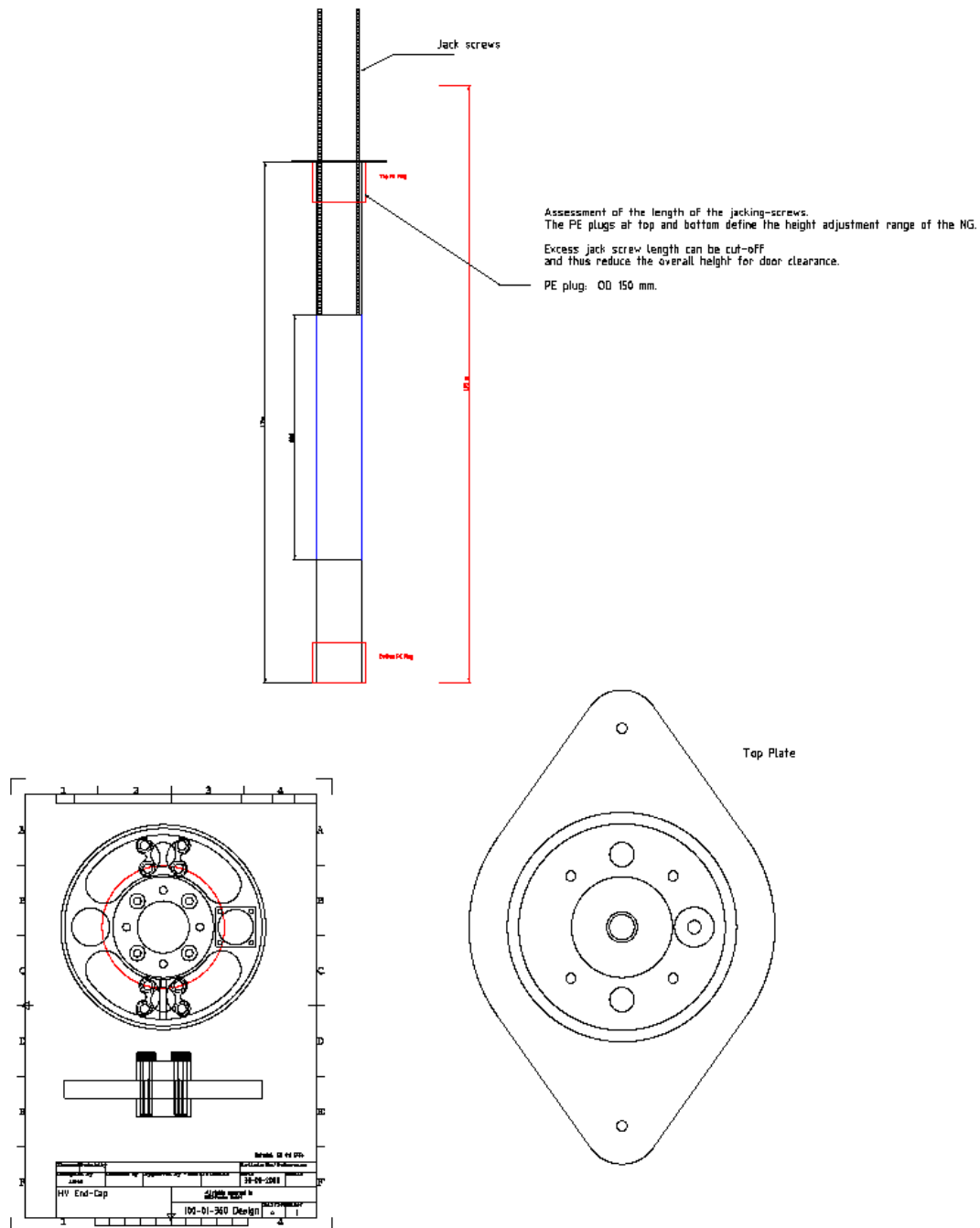


HS Mannheim laboratory

3.3 Vertical Support Sub-system

The following drawing indicates the main design features of the jack screw system.

Two Polyamide M16 threaded rods carry the 15 kg mass of the reaction chamber assembly.
 A wing nut holds each threaded rod.



The threaded rods are attached to the reaction chamber by means of the fixtures shown above left. The threaded rods are captured by means of M3 bolts which serve as a redundant fixture within the M16 attachment.

The M16 wing nuts sit on the top plate shown at right.

The Top Plate sits on the top of the shielded housing.

To it is attached the Polyethylene Top Plug assembly. This has a split construction which allows it to be installed over the already terminated High Voltage cable and the Low Voltage cable. The connectors fit through the holes in the Top Plate.

3.4 Mobility Requirement

A mobile or easily movable neutron and associated radiation shield has been included in the system specification.

The detailed requirements for this article have been tasked on NSD-Fusion to achieve best practice within the available budget and within the allowable dimensions.

3.4.1 Allowable Dimensions

A maximum diameter of 90 cm for the housing has been specified. This is mainly to limit the mass.

The height is to be limited to 2 m for doorway clearance. The width is limited to 1 m.

Access to the CERN laboratory is via double doors.

3.4.2 Mobility

The general assumption has been that the shielding will have a mass of approximately 1500 kg. In order move such a mass suitable equipment is required.

Option 1

A base frame with wheels can be envisaged. The frame would be fabricated from steel sections and fitted with swivel wheels in order to provide mobility within a laboratory building with suitable floor structure and access via a freight elevator.

Option 2

A base frame as mentioned above but without wheels which is configured as a pallet. For mobility a standard pallet lifter unit would be employed.

A trade-off matrix is presented below.

<i>Options</i>	<i>Wheeled Base</i>	<i>Pallet Base</i>
9 min. height 85 mm swivel castors for 2000 kg (<222 kg load)		
Polyamide Ball Race 1200 kg	90 x 9 = 810 Euro	
Polyurethane Bandage on Metal Wheel 700 kg	101 x 9 = 909 Euro	
Pallet Lifter 2500 kg, minimum height 85 mm, max. lift height 200 mm		250 Euro cheapest, 400 Euro better quality
Housing height adjustment	use a pallet lifter and blocks	use a pallet lifter and blocks under pads
Housing position adjustment	push the castors until they align and then steer the moving mass	pallet lifter access from four sides and at small angles
Locking in position	Small height castors are not available with breaks	Set down on pads
Locking in position	Large castors add height - reduce maximum housing height	
Fine height adjustment	Neutron generator jack screws	Neutron generator jack screws

The pallet lifter option offers greater flexibility.

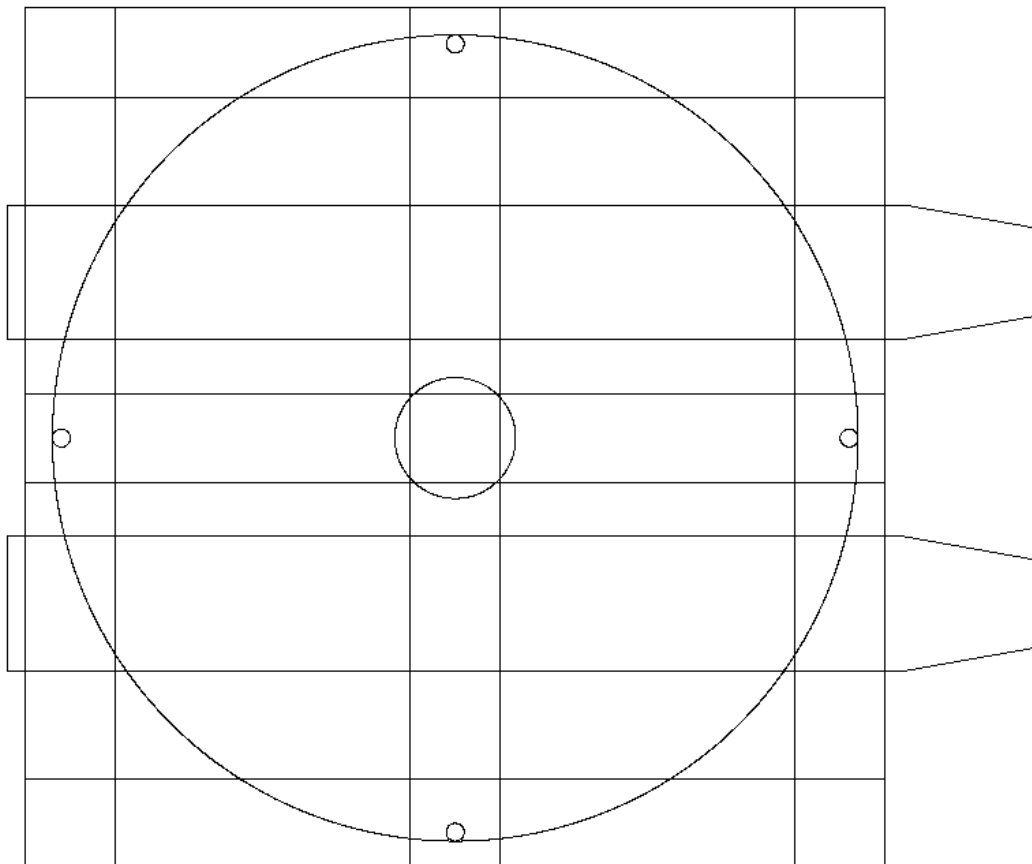


The unit pictured here can lift 2500 kg. Likely price ~270 Euro.

The shielding is a stable and symmetric load for such a pallet lifter.

3.4.3 Base Design

A maximum access pallet base shall be fabricated. Pallet lift fork or fork lift vehicle compatibility will permit fabrication, assembly and test at the NSD-Fusion facility, loading and unloading during transport to CERN, mobility in the CERN laboratory building and fine adjustment of position within the laboratory.



The steel pallet base will be fabricated from 100 x 50 mm cold rolled steel box section. The feet will provide a 100 mm clearance for the pallet lifter to be positioned.

In order to provide a crane lifting capability, four steel rods of 20 mm diameter will be installed on the steel pallet. These rods will have threaded ends. At the top each will be fitted with a DIN 582 "Ringmutter" or Ring Nut. Each is rated to carry 1.2 metric ton.

The rods will be stabilized at the top by a cross beam to ensure that rod spacing is maintained in the event of a lifting harness that does not have spacer bars.

3.4.4 Top of housing equipment

On top of the 180 cm shielding there will be space for:

- The height adjustment jack screws
- The air blower.
- The cooling air input and output 70 mm hose connections.

The high and low voltage cables can be configured and secured with due attention to the protection of these cables.

3.5 MCNP Model

In order to provide optimal radiological protection capabilities, a Monte Carlo analysis was carried out using the radiation transport code MCNP5¹ (Monte Carlo N-Particle).

3.5.1 MCNP Model Geometry

A detailed geometry model was built reproducing the geometry and materials of the NSD-NG, and surrounded by a cylindrical shield of diameter 90cm and height 1.8m. The NSD-NG is located on the axis of the cylindrical shield, and can be moved to various positions along this axis within a bore which is slightly larger than the NG OD. A minimum of 30cm shielding material is provided at each end of the bore. It is assumed that, for the present application, the NSD-NG will be mounted vertically, with power cables entering approximately axially from above; appropriate cabling and feed-throughs are modelled in detail within the Monte Carlo study. Air ducting is required within the shield assembly to provide a throughput of sufficient cooling airflow to the NSD-NG (see section 3.1 above); this ducting occupies a small but non-negligible fraction of the shield cross-section, and therefore must also be represented appropriately in order to ensure that this does not result in a radiological weak point in the design. It is proposed that four long steel rods be installed, equally spaced around the shield circumference, in order to provide a guarantee of structural integrity and to lock the assembly in place (“Vertical support sub-system” - see section 3.3 above). These, together with a small air-gap around each rod, are also included in the model.

Additionally, a neutron beam exit port is located adjacent to the thin aluminium neutron “beam window” of the NSD-NG. At present, this exit port is the basic design: A square cross-section hole of side 10cm x 10cm, and positioned radially from the NSD-NG neutron beam window to the outside of the shield. The modular design of the NSD mobile shielding enclosure permits the retrofitting of enhance collimator modules, for example to optimise the delivered neutron spectrum characteristics, or to limit the output beam dimensions as required.

The detailed geometry of the NSD-NG internal engineering design is not discussed here. However, an extended source distribution reflecting the known NSD-NG source region geometry and characteristics is used for the radiological study.

3.5.2 MCNP Material Definitions

Note that, throughout, material definitions are specified using isotopic (rather than elemental) cross-sections. In each case, all naturally occurring isotopes of each element are including, in the appropriate natural relative abundances. This is highly desirable for modelling of neutron-gamma photon production processes.

¹ “MCNP – A General Monte Carlo N-Particle Transport Code”, Los Alamos National Laboratory

3.5.3 Candidate Materials for the Radiation Shield

An extensive range of materials was considered in order to optimally meet the requirements of the current application. First and foremost, it is necessary to moderate the fast neutrons emitted from the NSD-NG, and then capture the resulting thermalised neutrons. Since we are dealing here with neutrons from dd fusion (as opposed to higher energy dt neutrons), we will best achieve moderation using light elastic scatterers. At much higher energies, such as for 14MeV dt neutrons, it can be more effective to initially reduce the neutron energy using inelastic scatterers such as carbon or oxygen; however, as these nuclei have inelastic scattering thresholds well above the energy of dd neutrons, this approach is inapplicable here. Therefore, the most effective materials will be hydrogen rich solids; these also offer strong thermal neutron absorption via hydrogen capture – a topic which will be revisited shortly.

Traditional neutron shielding materials, including paraffin, while providing good moderation and absorption of neutrons, have less than optimal mechanical and structural properties, and in the present application, it is desirable that the entire structure be physically robust. A number of materials, including plastics such as polyethylene (PE), were considered. However, a particularly appealing product which is now being used for neutron shielding is Water Extended Polymer (product name STEP 2, from Scott Bader), known as “WEP”. This offers good neutron moderation and absorption due to its hydrogen content, but also permits moulding into appropriate shapes, curing to yield a strong solid. Another highly attractive property is the ease with which additives can be blended into the WEP mixture, for example if required to enhance radiological transport properties (see below). After comparison with other candidates, it was decided that WEP would form the optimal base component of the shield.

Therefore, an initial simulation was performed for the NSD-NG neutron generator located within a cylindrical shield of pure WEP (density 1.08g/cc) of diameter 90cm and height 1.8m, with the NG source point assumed to be midway up the shielding cylinder axis. Note that, due to the internal construction of the NSD-NG, this does not result in exactly equivalent shielding at the top and bottom of the cylinder (in fact, a slightly higher degree of radiation shielding is provided in the upward direction due to ceramic components above the neutron source electrode region).

Advanced features of MCNP, including the mesh tally option, were exploited to generate a radiation flux and dose rate map over the curved surface of the cylindrical shield, as well as over each end of the shield. A range of variance reduction techniques were deployed in order to optimise statistical precision. Through this study, both neutron and photon fields are expressed, unless otherwise noted, as biological dose equivalent rates in Sv/h (or more usually, due to the low residual dose rates achieved, in $\mu\text{Sv/h}$) using the ANSI/ANS-6.1.1-1977 conversion factor parametrisation, and assuming a neutron source output rate of 2×10^7 n/s (DD) as called for by the present application. The term “dose rate” will be used interchangeably with “biological dose equivalent rate” unless otherwise specified.

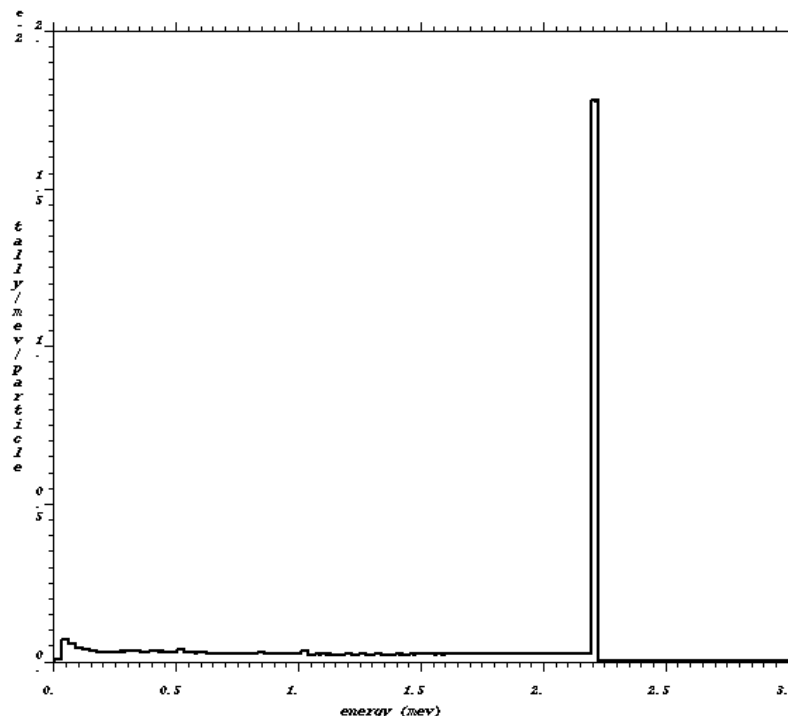
Furthermore, note that the present discussion relates to photon dose rates arising from secondary gamma-rays generated by (n, γ) reactions – both neutron inelastic scattering and neutron capture. Photon dose rates from Bremsstrahlung within the neutron source electrode are subject to additional dependences and are discussed separately (below).

The initial models showed a maximum field for both neutrons and photons around the circumference of the shield in the plane of the neutron source region and collimator. The fields decreased for axial positions closer to the ends of the shield, and the top and bottom of the shield exhibited significantly lower fields for every case studied. Therefore, throughout this report, with the emphasis on radiological protection, the “worst case” fields close to the source point are quoted. These are averaged over a band around the cylindrical surface of the shield, of width $\pm 20\text{cm}$ either side of the centre of the neutron source electrode region and collimator exit, but excluding the neutron beam exit hole and immediate surround. Dose rates around the circumference of the cylinder (at a fixed height) vary moderately, which is ascribed to the presence of air ducts and other non-axially symmetric structures; however, this variation in rate is small compared to the average value of the dose rate.

The initial model, with shield consisting only of WEP (density 1.08g/cc), provided an estimated maximum neutron dose rate of $3.03\mu\text{Sv/h}$, and an estimated maximum photon dose rate of $7.17\mu\text{Sv/h}$.

Thus, of a total (maximum) dose rate at the surface of the shield of $10.2\mu\text{Sv/h}$, over 70% of the dose arises from photons (rather than neutrons). We note also an earlier comment from CERN that “there is a considerable amount of gamma radiation produced”. As a result, additional optimisation effort was deployed in an attempt to reduce the surface photon field still further.

First, it is important to consider the mechanisms giving rise to this γ -ray field. The simulated γ -ray energy spectrum for a small test region close to the shield at the region of maximum field is shown below for the case of a shield comprising only WEP:



As can be seen unambiguously, the photon spectrum at the surface of the shield is overwhelmingly dominated by the 2.22MeV hydrogen (thermal neutron) capture line at 2.22MeV, together with background arising from scattering of this line. (Note that the plot shows the surface flux spectrum *converted to dose equivalent rate* and therefore does not

show precisely the same shape as a γ -ray energy spectrum as measured by a spectroscopy detector; furthermore, structures below full-energy normally seen in measured spectra due to scattered photons escaping the detector are also absent; and finally, no detector resolution effects are folded into this modelled dose spectrum).

Note that, because of the relatively low neutron energy produced in dd fusion, there is virtually no inelastic photon production. Other than a trace presence of N and Sn (at about 0.1%wt levels or below), WEP consists of C, O and H. For obvious reasons, H does not give rise to inelastic scattering γ -rays, and carbon and oxygen have inelastic scattering thresholds above the dd neutron energy due to their high-lying first excited states. Therefore, the neutron-induced photon spectrum (i.e. the photon spectrum other than from source Bremsstrahlung) arises predominantly from thermal neutron capture for a dd source.

This important aspect is also reflected in another feature of the simulated radiation fields: Analysis of the neutron dose rate spectrum for the WEP shielding shows that only 1.08% of the surface dose, as measured in the region of maximum field on the curved surface of the shield close to the NSD-NG source electrode region, arises from thermal neutrons, while almost 99% arises from fast neutrons. (For the purposes of the present study, the epithermal neutron regime – typically considered to be the energy range 0.2eV to 10eV – is included in the category of “thermal” neutrons, and fast neutrons are taken to be those of energy 10eV and above.) Thus we see that, unsurprisingly, most neutrons which are moderated to thermal (or epithermal) energies are then captured within the shield, giving rise to capture γ -ray emission.

In order to reduce the photon radiation field at the surface of the shield, therefore, we have two options: (a) increase shielding to further suppress these γ -rays, or (b) reduce the rate of thermal capture on hydrogen.

Considering the first option (a): Due to the high energy of the hydrogen capture line, we note that interaction of these 2.2MeV photons with matter in the shield will be predominantly via Compton scattering. The Compton scattering cross-section varies approximately with the atomic number of the scattering nucleus, Z , and shielding efficiency increases roughly with the mass density of the shielding material. Thus it will be helpful to increase the shield density. However, we are heavily constrained in this regard, since it would be counter-productive to reduce the hydrogenous content of the shield, leading to an increase in neutrons reaching the outer part of the shield – potentially increasing both neutron *and* photon fields at the surface of the shield. However, it is possible to consider either small amounts of additives, or somewhat greater fractions of materials with significant hydrogen content; these options may offer a modest improvement in γ -ray shielding efficacy.

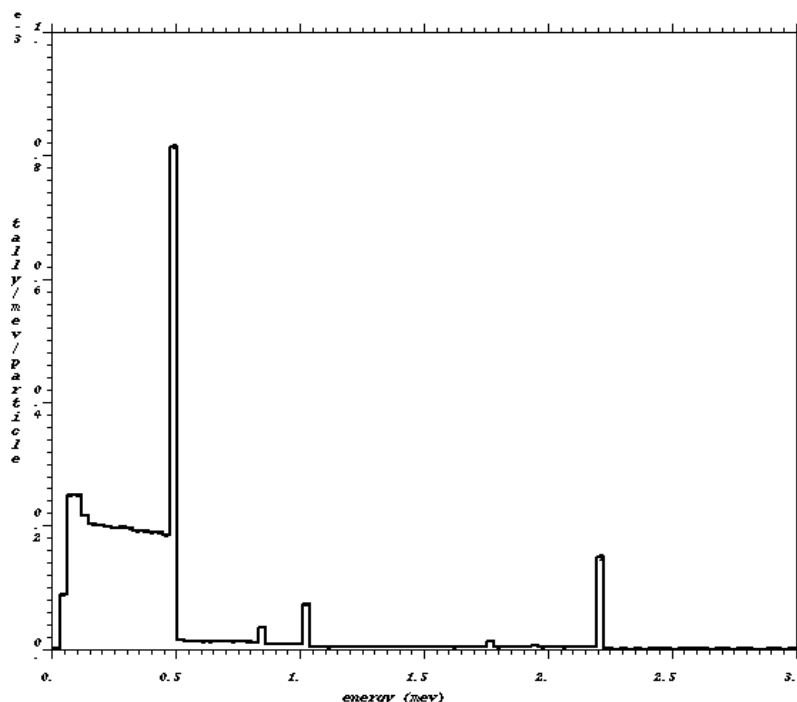
Option (b) offers alternative and more hopeful prospects: By reducing the rate of thermal capture on hydrogen, we reduce the rate of production of these highly penetrating 2.22MeV capture γ -rays correspondingly. However, we wish to reduce neither the neutron output from the NSD-NG, nor the hydrogen content of the shield, since this is required to achieve moderation of the initial fast neutron flux. How then can we reduce the rate at which thermal neutrons are captured by hydrogen? Instead, we propose adding boron-containing additives to the shielding material. Boron-10, which comprised 20% of naturally occurring boron, is an extremely effective absorber of thermal neutrons; indeed, the macroscopic thermal absorption cross-section Σ (the atomic cross-section multiplied by the number density of atoms per unit volume) for boron is more than 200 times greater than that of hydrogen. The effect of a small

addition of boron is therefore to preferentially “mop up” thermal neutrons via capture on boron instead of via hydrogen capture (although some residual hydrogen capture will of course still take place). This not only means that the thermal flux is more rapidly suppressed, and therefore covers a smaller extent from the neutron generator, but crucially, capture on boron leads to the emission of a much lower energy capture γ -ray of energy 478keV (and only with a 94% branching ratio) instead of the 2.22MeV γ -ray emitted by hydrogen. This in turn means that the resulting flux of capture γ -rays, which is unavoidable if the thermalised neutrons are to be absorbed, is now of very much lower energy, and therefore very much more strongly attenuated by the NSD-NG shielding material.

An acceptable way to add boron is via the addition of the naturally occurring mineral Colemanite ($\text{CaB}_3\text{O}_4(\text{OH})_3 \cdot \text{H}_2\text{O}$). Tests performed by NSD-Fusion show that this can be easily incorporated into the WEP mixture without compromising structural integrity. Additionally, Colemanite has a relatively high mass density (2.4g/cc), which will help to maintain the shield density and therefore assist with attenuation of γ -rays in the Compton scattering energy domain (~100 keV up to several MeV, typical of those produced by neutron inelastic scattering and capture). Finally, when source Bremsstrahlung radiation is discussed below, it will be noted that Colemanite also contains approximately 20%wt Calcium (atomic number $Z=20$), which will greatly enhance suppression of Bremsstrahlung photons (in the photoelectric “PE” energy domain below ~100keV, where absorption cross-section depends approximately on Z^4). Particularly desirable is the significant fraction of hydrogen within Colemanite – although only just over 2%wt, this is much lower than the hydrogen fraction in WEP (9%wt), but still preferable to the largely hydrogen free alternative sources of boron. For comparison, one such material, diboron trioxide (B_2O_3) will be considered below.

In addition to the pure WEP shield composition, therefore, MCNP models were also run for mixtures of WEP with 25%wt and 50%wt Colemanite, noting that higher Colemanite fractions are likely to compromise the structural integrity of the shield (as well as reducing the hydrogen content unacceptably), therefore limiting the amount of boron which can be added via Colemanite (which contains approximately 13%wt boron). In order to assess the benefits of further boron enrichment, therefore, five further cases were modelled, in which 10%wt of B_2O_3 (31%wt boron) was substituted for an equivalent mass fraction of either WEP or Colemanite.

The impact on the γ -ray field due to the addition of boron is striking. The figure below shows the surface dose spectrum, exactly comparable to the above figure for WEP and for the same neutron generator output, but in this case for a 50/50 mixture (by weight) of WEP/Colemanite:



Note the change of scale on the y-axis – the maximum bin dose is now around 20 times lower than before, and is at 0.478keV instead of 2.22MeV as before. The hydrogen capture peak at 2.22MeV is still visible, but reduced in yield by approximately 2 orders of magnitude. The effect of replacing the highly penetrating 2.22MeV capture γ -ray yield by the much “softer” (and therefore much more strongly attenuated) 478keV line is also reflected in the calculated maximum photon dose rate at the surface of the shield, which drops from 7.17 μ Sv/h to only 0.54 μ Sv/h. Significantly, the photon flux now contributes only ~13% of the total surface radiation field, instead of over 70%, and thus the total radiation field at surface falls from 10.2 μ Sv/h to only 4.3 μ Sv/h.

At this point, it is worth remembering that, as pointed out earlier, the overwhelming part of the neutron dose rate at surface arises from fast neutrons. For pure WEP, this fraction is almost 99%, and this rises still further with any addition of thermal-neutron-suppressing boron. Therefore, we should not expect the addition of boron to substantially decrease the neutron dose rate (since boron suppresses primarily thermal neutrons, which contribute only negligibly to the total neutron dose rate). However, the replacement of hydrogenous material by boron-rich (but non-hydrogenous) materials may well lead to less effective moderation of fast neutrons, and therefore a net increase in neutron dose rate.

3.5.4 Dose Rate Simulation Results

The following table gives the estimated neutron, photon and total dose equivalent rates (in μ Sv/h) which would be expected at the surface of the shield in the region closest to the NSD-NG source region (but not including the flux via, or very close to, the neutron beam exit). This is the region of highest radiation field for each modelled case.

The table lists 8 different proposed shielding material compositions, labelled for convenience by names reflecting the mixture components: All start with “W”, indicating the base component, WEP. The letter “C” (if present) followed by a number indicates the corresponding weight percentage of Colemanite; and the letter “B” represents an addition of 10%wt of B₂O₃. These compositions are also specified in the table. The density used in the

model for each mixture is given in g/cc. Finally, the right-hand columns show the predicted dose rate for neutrons, photons, and the total (n+p). Estimated statistical uncertainties are computed but not listed here for conciseness: However, statistical uncertainty for both neutron and photon dose rate estimates are approximately 1% in all cases, and are therefore considered lower than uncertainties arising from non-statistical effects (e.g. variations in material specifications or other experimental conditions).

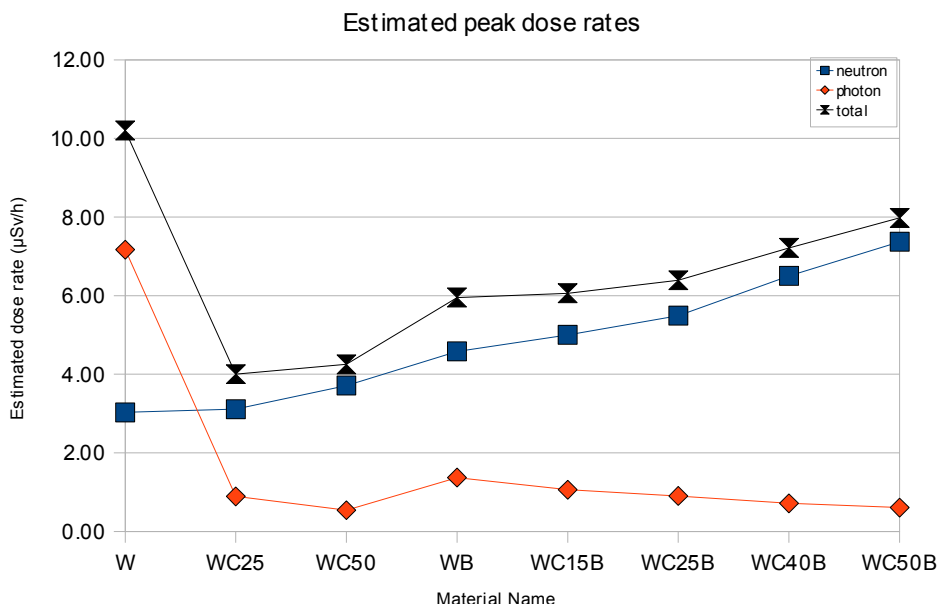
NB: This table, and the accompanying discussion, refers only to photons generated by (neutron,gamma) reactions, specifically by neutron capture and scattering. This section does NOT include radiation fields arising from Bremsstrahlung effects taking place within the neutron generator, which has other dependencies and will be discussed separately below.

Name:	Mixture fractions by weight%			Mixture density (g/cc)	Average peak dose rate ($\mu\text{Sv/h}$)		
	WEP	Colemanite	B ₂ O ₃		neutron	photon	total
W	100	0	0	1.0800	3.03	7.17	10.20
WC25	75	25	0	1.2522	3.11	0.89	4.00
WC50	50	50	0	1.4897	3.71	0.54	4.25
WB	90	0	10	1.0805	4.58	1.37	5.95
WC25B	65	25	10	1.2528	5.49	0.90	6.39
WC50B	40	50	10	1.4906	7.37	0.61	7.98
WC15B	75	15	10	1.1777	5.00	1.06	6.06
WC40B	50	40	10	1.3854	6.50	0.71	7.21

Immediately we note certain key features: In particular, that for WEP alone, the photon dose rate of $7.17\mu\text{Sv/h}$ is more than twice that from neutrons, and leads to a total dose rate at surface of up to $10.2\mu\text{Sv/h}$. However, for all additional amounts of boron (from 10%wt of B₂O₃ up to the most boron-loaded case, with 50%wt Colemanite and 10% B₂O₃), the photon dose rate drops sharply to around $1\mu\text{Sv/h}$. This strongly suggests that the addition of a small amount of boron will prove extremely effective in mopping up thermal neutrons, and preventing them from producing highly-penetrating 2.22MeV hydrogen capture γ -rays.

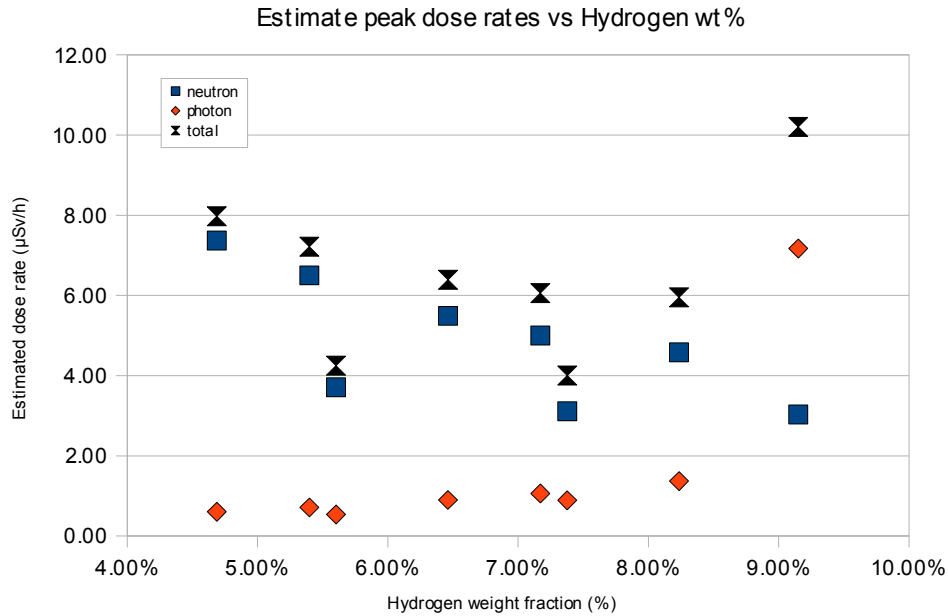
The neutron, photon and total dose equivalent rates are plotted below. The first 3 points, labelled “W”, “WC25” and “WC50” are pure WEP and WEP with the addition of 25%wt and 50%wt Colemanite. In order to maintain optimal structural properties, it is desirable to keep the fraction of Colemanite at below 50% by weight, and therefore higher fractions were not simulated. The addition of 25% Colemanite clearly strongly reduces the photon radiation dose at the shield surface, via the thermal neutron absorbing boron content. The neutron dose rate increases very slightly. For the 50/50 WEP/Colemanite mixture “(WC50)”, it is noted that the photon dose rate is reduced somewhat further, but this is now at a cost of increasing neutron dose; indeed, the net total dose (neutron plus photon) increases slightly as the Colemanite fraction is increased from 25%wt to 50%wt. This is because, while the boron absorbs thermal neutrons which otherwise contribute strongly to photon radiation via the hydrogen capture 2.22MeV γ -ray, these thermals in any case contribute little (around 1% or less) to the neutron dose rate as measured at surface. However, the substitution of boron-containing Colemanite for WEP is accompanied by a reduction in the hydrogen content of the mixture, since WEP is considerably more hydrogen-rich than Colemanite. The fast neutron flux at surface (which constitutes around 99% or more of the total neutron dose) therefore actually *increases* - somewhat counter-intuitively - with the addition of the (thermal) neutron-absorbing boron.

Noting that the total dose rate curve is approximately flat between the two WEP/Colemanite points (“WC25” and “WC50”), we may take this range of mixtures as a suitable candidate specification for optimal shielding. We will return to this later.



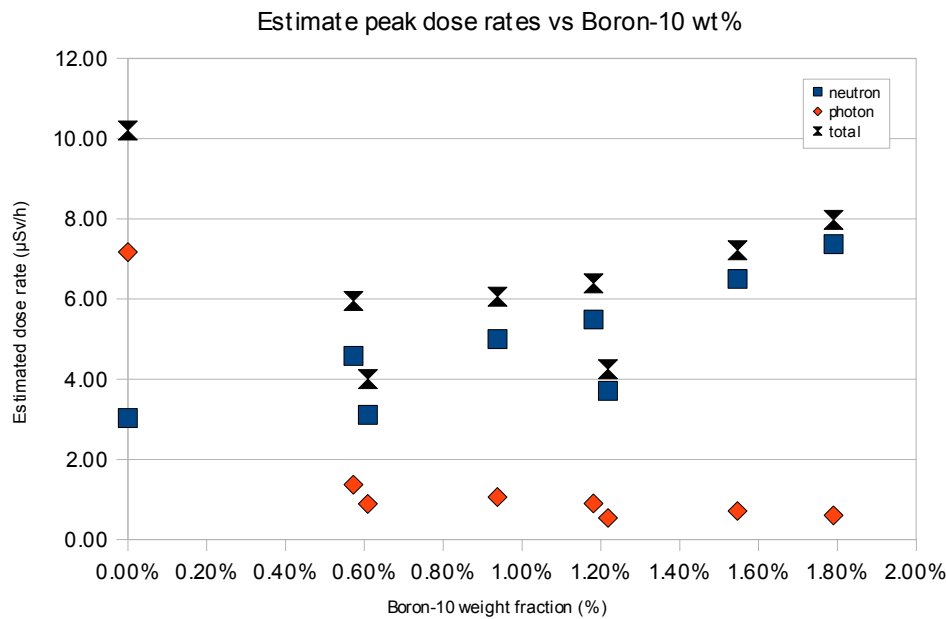
Clearly, the mixtures in which WEP or Colemanite has been replaced by 10%wt B₂O₃ exhibit higher neutron dose rates. However, little has been gained in terms of photon dose rate compared to WEP/Colemanite mixtures. This is due to a number of factors. Firstly, boron has such a large thermal capture cross-section (compared to hydrogen) that relatively little boron is required to dominate the thermal capture processes taking place within the shield. The addition of further boron therefore is subject to the law of diminishing returns. However, the added diboron trioxide is displacing hydrogenous WEP or Colemanite, so that the neutron dose rate – which is dominated by fast (not thermal) neutrons – increases due to less effective moderation. Additionally, diboron trioxide has a much lower density (1.085g/cc) than Colemanite (2.4g/cc), so that the attenuation of neutron-generated γ-rays, which takes place primarily via the Compton effect, is weaker than for higher density mixtures with greater proportions of Colemanite.

Further insight can be gained by plotting the simulated rates as a function of the hydrogen weight fraction in the mixture, as below. As expected, the neutron dose rate decreases with increasing hydrogen fraction. Note that the points for WEP and WEP/Colemanite (lowest three neutron dose rate points, below 4.0μSv/h) do not fall on the same trend as the five points containing diboron trioxide. This is not surprising, for a number of reasons. In particular, other elemental compositions are changing – for example, the fraction of Carbon is approximately 37% in WEP, but only 1.5% in Colemanite and absent in boron trioxide. Carbon is one of the lightest elements present, after hydrogen, and contributes somewhat to moderation of fast neutrons. A clear example of such misleading trends can be seen in the photon dose rate data, which appear to show an increase in photon dose with increasing hydrogen fraction; in fact, this is of course an indirect reflection that the highest hydrogen fractions occur in mixtures with the lowest proportion of the hydrogen-free B₂O₃, and it is in fact the lack of boron (not the increase in hydrogen) which results in high photon dose rates.



The mirror image of this effect is seen in the next graph, which shows the dose rates as plotted against boron-10 fraction (boron-10 constitutes just under 20% of natural elemental boron). Here, the photon dose rate is now seen to be clearly decreasing with added boron, particularly for the addition of the first 0.6%wt fraction of boron-10. The neutron dose rate appears to increase with increasing boron – actually a reflection of *decreasing* hydrogen content.

It is noticeable that there are two pairs of points with very similar boron content but different dose rates, at approximately 0.6% boron-10 and approximately 1.2% boron-10. These correspond to different combinations of Colemanite and diboron trioxide as the source of boron. In the first pair, at ~0.6% boron-10, the lower dose rate point is the mixture of WEP and 25%wt Colemanite; the upper (higher dose rates) point is 90%wt WEP with 10% boron trioxide. Clearly, the mixture with Colemanite is more effective in shielding both neutrons and photons. This is at first surprising, since the mixture with Colemanite actually contains a lower weight percentage of hydrogen. However, this is not the full story: The Colemanite mixture also has a significantly higher density (over 1.25g/cc instead of 1.08g/cc). As a result, the hydrogen *density* (ie g/cc of hydrogen) is in fact roughly the same for both cases at around 90%, meanwhile, the boron *density* (g/cc of boron-10) is significantly higher for the WEP/Colemanite mixture at 7.6mg/cc than for the WEP/B₂O₃ mixture (6.2mg/cc).

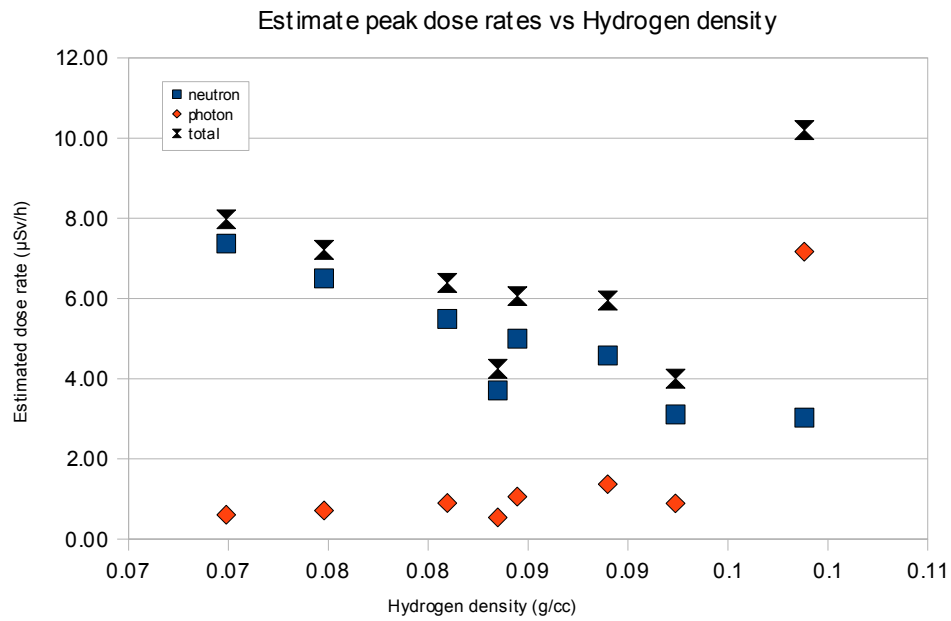
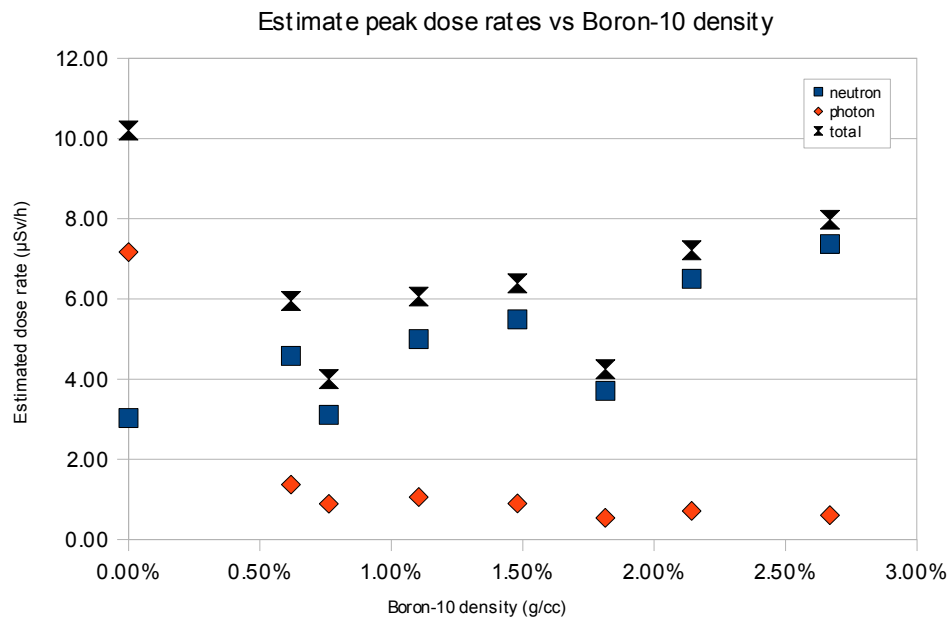


This point is illustrated even more starkly for the pair of points at ~1.2% boron-10 weight fraction, which are a 50/50 mixture of WEP/Colemanite (lower point for neutron, photon and total dose rates) and a mixture of WEP/Colemanite/B₂O₃ in the weight proportions 65/25/10. If the dose rates are plotted against the boron density (mass of boron-10 per cc) instead of weight fraction, and therefore taking account of changes in mixture density, these two points now appear at boron-10 *densities* of 1.81g/cc (lower dose rate points) and 1.48g/cc (higher dose rate points).

A similar exercise is carried out for hydrogen, by plotting neutron, photon and total dose rates against hydrogen density (mass of hydrogen per cc of mixture). Here again, a noticeably more consistent trend is observed than when plotting dose rates against only hydrogen weight fraction.

The important point is that, in making any change to the mixture, a number of properties will necessarily be simultaneously changed, since no single element can be changed in isolation. Important properties of the mixture will be the following:

- hydrogen density (and to a lesser extent, presence of other light elements) for moderation of fast neutrons – this will principally affect the neutron dose rate;
- boron density to absorb thermal neutrons preferentially in place of hydrogen capture – this will principally affect the *photon* dose rate;
- mixture density will influence both of the above, and higher mixture densities will additionally afford greater attenuation of neutron-induced γ -rays;
- finally, the presence of comparatively high atomic number elements will improve the attenuation of low-energy photons (below approximately 100keV); this will be relevant when discussing Bremsstrahlung radiation (see below). Colemanite contains almost 20%wt of Calcium with atomic number $Z=20$ – higher than any other element (other than trace quantities) in any of the shielding materials.



3.5.5 Bremsstrahlung

As part of the radiological assessment, it is necessary to consider the photon dose rate arising from Bremsstrahlung in the NSD-NG high voltage electrode region. The Bremsstrahlung production rate depends on a number of factors which are not yet specified for the present deliverable system, and therefore it is not possible to simulate absolute dose rates due to Bremsstrahlung. However, it is possible to simulate the efficiency of the shielding enclosure as a means to suppress Bremsstrahlung radiation fields. This information can later be used, together with measurements of the Bremsstrahlung field from an unshielded NSD-NG, to deduce the residual photon dose rate arising. Two simulations have been performed: First, representing the Bremsstrahlung spectrum by an 80keV photon source, and secondly, as an absolute “worst case” to provide an upper limit to the Bremsstrahlung external dose rate, using a 120keV (line) photon source. In practice, the Bremsstrahlung spectrum will be a continuum from an end point at or below the NSD-NG HV energy down to effectively zero, and therefore will be suppressed more effectively than the line source model suggests. However, for a safety assessment, using a worst case scenario is appropriate.

The same geometrical models as above were used to estimate the shielding efficiency for Bremsstrahlung fields in the same peak dose region, around the circumference of the cylindrical shield close to the neutron source position.

Given the analysis presented in section 3.5.4 above, it seems clear that the addition of diboron trioxide has no benefit for the present application. Therefore, we focus our attention on combinations of WEP and Colemanite. The figures below are for the 80keV assumed source, with the corresponding figure for a 120keV “worst case” source in parentheses ().

The following table shows the estimated external residual photon flux and dose arising from Bremsstrahlung relative to an unshielded NSD-NG (measuring at the same position outside the shield). Note that the suppression factors for flux and dose are not identical, since the shield alters the energy spectrum of the transmitted photons. As expected, the 120keV source is less well attenuated than the 80keV source. As before, these quantities are calculated to a precision of around 1%.

WEP+...	Assuming 80keV line photon source		Assuming 120keV line photon source	
Colemanite Fraction	Residual relative flux	Residual relative dose rate	Residual relative flux	Residual relative dose rate
0%	2.52×10^{-2}	3.25×10^{-2}	5.96×10^{-2}	6.25×10^{-2}
25%	3.19×10^{-3}	3.48×10^{-3}	1.38×10^{-2}	1.29×10^{-2}
50%	3.83×10^{-4}	3.96×10^{-4}	3.00×10^{-3}	2.75×10^{-3}

It was noted earlier that a shield consisting of WEP with a Colemanite fraction in the range 25-50%wt would be optimal for minimisation of the neutron and photon fields arising from source neutrons, with a weak preference for somewhat lower Colemanite fractions (i.e. nearer to 25%) if neutron fields are of concern, although the effect is small. Clearly, if shielding the residual Bremsstrahlung field is particularly important, then a somewhat higher Colemanite fraction (of around 40%wt or higher) could be advantageous.

Note that, in the special case of Bremsstrahlung, very effective additional shielding techniques can be supplied. Relatively thin sheets of heavy metal (such as lead) can be wrapped around the NSD-NG body close to the source, effectively suppressing the Bremsstrahlung field. A hole would then be cut in the lead foil in front of the aluminium “neutron window” in the NSD-NG housing. Since the Bremsstrahlung is of energy below around 100keV, it will interact predominantly via the photoelectric effect (rather than by Compton scattering), and therefore will be confined to a “fan” close to the solid angle subtended by the neutron exit window. Therefore, further lead foil can be supplied on the outer surface of the WEP/Colemanite shield close to the neutron beam exit (or collimator). This will very effectively suppress any residual Bremsstrahlung photons.

3.5.6 Shielding Radiological Study Conclusions

A detailed Monte Carlo analysis has yielded the following conclusions:

- For suppression of the neutron dose rate external to the assembly, a shield consisting of WEP with an added Colemanite fraction in the range 25-50% offers excellent properties. If neutron dose rate is the sole criterion, then a Colemanite fraction towards the *lower* end of this range is marginally preferred.
- For suppression of the secondary photon dose rate resulting from neutron capture and scattering, the same shield composition is optimal. If photon dose rate is the sole criterion, then a Colemanite fraction towards the *higher* end of this range is marginally preferred.
- Taking the total radiological dose equivalent rate (including neutrons and photons), then a shield composition anywhere in the above range offers approximately similar shielding efficacy.
- If the residual field from Bremsstrahlung radiation produced in the NSD-NG is a concern, then a Colemanite fraction in the upper part of the above range would be effective in improving attenuation of the Bremsstrahlung flux. However, alternative targeted techniques for reducing this low-energy photon radiation may be preferable.

Note: The above Monte Carlo analysis is intended as guidance for design purposes only. The dose rate estimates provided should not be used for radiological purposes.

4 Conclusion

The operational safety features of the NSD neutron generator take into account the interfaces required by radiation safety regulations and the considerations of ALARA (As Low As Reasonably Achievable).

The addition of a shielding housing constrained to be mobile as defined above has been a new design exercise. The employment of MCNP as a design tool has been combined with a pragmatic cost minimization design study to achieve the customers requirements.

The shielded housing will be duplicated for NSD-Fusion's own usage within its new manufacturing and test facility. Fabrication of the shielded housing and subsequent integration of the neutron generator and dosimeter equipment can now proceed.